RESEARCH ARTICLE

Industrial Fermentation

Biotechnology Journal

www.biotechnology-journal.com

Computer Simulation Elucidates Yeast Flocculation and Sedimentation for Efficient Industrial Fermentation

Chen-Guang Liu, Zhi-Yang Li, Yue Hao, Juan Xia, Feng-Wu Bai, and Muhammad Aamer Mehmood**

Flocculation plays an important role in the immobilized fermentation of biofuels and biochemicals. It is essential to understand the flocculation phenomenon at physical and molecular scale; however, flocs cannot be studied directly due to fragile nature. Hence, the present study is focused on the morphological specificities of yeast flocs formation and sedimentation via the computer simulation by a single floc growth model, based on Diffusion-Limited Aggregation (DLA) model. The impact of shear force, adsorption, and cell propagation on porosity and floc size is systematically illustrated. Strong shear force and weak adsorption reduced floc size but have little impact on porosity. Besides, cell propagation concreted the compactness of flocs enabling them to gain a larger size. Later, a multiple flocs growth model is developed to explain sedimentation at various initial floc sizes. Both models exhibited qualitative agreements with available experimental data. By regulating the operation constraints during fermentation, the present study will lead to finding optimal conditions to control the floc size distribution for efficient fermentation and harvesting.

1. Introduction

Flocculation is a reversible aggregation of thousands of cells to produce flocs via intercellular adhesion. It does not only offer a convenient way to harvest the biomass from the fermentation broth, but also enhances the cellular tolerance to various stresses including high ethanol concentration.[1,2] Various microorganisms take the advantage of flocculation such as yeasts,[3] bacteria,[4] and algae.[5] Since yeast flocculation has been utilized for a long time in the brewing industry for efficient and cost-effective biomass recovery instead of centrifugation,[6] molecular mechanism of yeast flocculation has been well studied. Flocculation involves molecular selective binding between sugar residues and lectin-like proteins on the surface of the cells. Multiple factors determine the flocculation including genetic basis, gene expression, and cell–cell interaction.[7]

The morphological characteristics of flocs have great influence on fermentation and separation.[8] The larger size and lower porosity of flocs offer easier separation of cells from the fermentation broth. Conversely, increasing floc size develops a mass transfer resistance inside the flocs and decreases porosity, which consequently causes the apparent reaction rate drop.[9] Therefore, it is essential to control mass transfer and sedimentation by regulating flocs structures.

Collisional flocculation of particles is caused by three transmission processes including perikinetic flocculation, orthokinetic flocculation, and differential settling.[10] Shear force is also involved when cells flocculate in bioreactors thus flocs establish an equilibrium between flocculation and disintegration forces. Moreover, live yeast cells proliferate in the flocs and new cells join into the floc as the older cells come out.

Morphological characteristics of flocculation have been mostly studied on mud, sand, and active sludge with rigid structures,[11–13] which can be analyzed by offline detection methods. Unfortunately, cell flocs are too fragile to sample, so off-line observation unavoidably destroys original structures of flocs and reflects the biased observations. The in-situ image analysis methods were developed to study size distribution.[14,15] For instance, Focused Beam Reflectance Measurement (FBRM) which uses a laser beam to scan all particles passing by the probe without any interference in the fermentation system, is a promising in situ approach to obtain the floc size distribution.[16–18] Other than FBRM, a digital imaging procedure has also been used to study floc size distributions established via flocculation and sedimentation under different operating

Dr. C.-G. Liu, J. Xia, Prof. F.-W. Bai, Dr. M. A. Mehmood
State Key Laboratory of Microbial Metabolism
School of Life Sciences & Biotechnology
Shanghai Jiao Tong University
Shanghai 200240, China
E-mail: cg.liu@sjtu.edu.cn; draamer@gcuf.edu.pk

Dr. Z.-Y. Li
School of Information Science and Technology
Dalian Maritime University
Dalian, Liaoning 116023, China

Dr. Y. Hao
Key Laboratory of Pollinating Insect Biology of the Ministry of Agriculture
Institute of Apicultural Research
Chinese Academy of Agricultural Sciences
Beijing 100093, China

M. A. Mehmood
Department of Bioinformatics & Biotechnology
Bioenergy Research Centre
Government College University Faisalabad
Faisalabad-38000, Pakistan

DOI: 10.1002/biot.201700697

conditions.[19] However, to understand the detailed structure of flocs is still difficult so far. Diffusion-limited aggregation (DLA) proposed by Witten and Sander has been the most extensively used model to study floc structures which perfectly simulated flocculation via the random collision of elementary particles.[20–22] However, the model could not provide proper analysis of experimental phenomena of flocculating yeast because of the growth of the live cell which should be involved in this model.

Moreover, various novel flocculation technologies have been developed to harness the potential of microbial flocculation in wastewater treatment and fermentation.[23] Previously, numerical simulations have been employed to predict the temporal variation of particle size distribution for cohesive sediments by using the quadrature method of moments (QMOM).[24] However, there are still several milestones and validations are critically essential to achieve the optimum utilization of the process.

The present study did not roughly correlate the floc size and other parameters by an empirical model,[25] but built up the simulation for flocs formation and sedimentation from which the flocs morphological characters can be analyzed to reflect the real flocs properties. In this study, a single floc growth model based on DLA was employed owing to its simplicity in computation and accuracy of results, along with FBRM to monitor in-situ structural characteristics of flocs. Experimental phenomena of most yeast flocs were elucidated. In addition, flocs growth during sedimentation was simulated using a multiple flocs growth model, and time-saving strategies for sedimentation were proposed.

2. Experimental Section

2.1. Growth Conditions

Flocculating yeast *Saccharomyces cerevisiae* SPSC01 (Accession number at, Chinese General Microbiological Culture Collection Center; CGMCC0587), was cultured in a 250 mL shake flask containing 100 mL modified YPD medium containing ($g\,L^{-1}$) yeast extract 4, peptone 3, dextrose 30. After inoculation, the shake flasks were put under constant shaking at 150 r min^{-1} for 18 h where temperature and pH were maintained at 30 °C and 4.5, respectively.

2.2. DLA Model of Flocculating Yeast

The procedure of DLA is shown in Figure S1, Supporting Information. Simply, to define the central point in a limited space as the "core cell" firstly; then a particle generated randomly on the margin moves in a Brownian manner, which makes the particle either absorbed by the flocs or drift out and vanish. Finally, the process is repeated as another particle being generated.

On the other hand, deflocculation should also be considered through the following principles: 1) Yeast cells located on the surface of the flocs are more vulnerable to shear force when compared to the cells at core; 2) A cell with maximum cell–cell connections is the most stable; 3) Disintegration of flocs includes detachment of single cell and crack of branches; 4) Interaction between cells is characterized by absorption factor a, when shear force acts upon a cell, it has a (1-a) probability to detach.

The two-dimensional (2-D) simulation of DLA was performed as it requires simple computation and provides enough accurate results.

2.3. Parameters of Simulated Flocs

Specific growth rate "μ" was defined as the ratio of the newly regenerated cells (N_{new}) to the total cells (N_{total}) over a certain period of time.

$$\mu = \frac{N_{new}}{tN_{cell}} \tag{1}$$

Simulated cell concentration (C_N) was defined as the ratio of cell numbers (N_{cell}) to total space area (S), which corresponds to cell dry weight (C, $g\,L^{-1}$) as depicted below:

$$C_N = 4 \times 10^{-3} \cdot \frac{C}{\rho_C} \tag{2}$$

ρ_C is for cell density, $g \cdot cm^{-3}$

The porosity (σ) of the flocs for particle diameter d is defined as equation 3.

$$\sigma = 1 - \frac{4N_{cell}}{\pi d^2} \tag{3}$$

2.4. Floc Porosity From Chord Length Distribution

The probe of Focused Beam Reflectance Measurement, FBRM (Model M400L, Lasentec, Redmond, WA) was inserted into the stirred fermenter to observe the chord distribution of yeast cell flocs. The biomasses of cells were adjusted to 0.6, 3.0, 6.0, 15, 20, and 60 $g\,L^{-1}$ (dry weight) as simulated cell concentration (C_N), and the rotation were controlled at 100, 200, 300, 400, 500, 600, and 700 r min^{-1}, which corresponded to absorption factor a as following empirical equation $a = -0.001^*$ rotation $+ 0.7$ (when rotation <700 r min^{-1}); $a = 0$ (when rotation $>=700$ r min^{-1}).

According to the manual of FBRM, 0–1000 μm range of chord length was divided into 500 linear sections, and the chord length distribution can be plotted with a median value (L_i) vs. count of chord length (b_i). Flocs usually bear fractal structures,[26] thus the relation of chord lengths of flocs and cell numbers can be expressed as a fractal equation:

$$N_{cell} = A_D L^D \tag{4}$$

where the A_D is the fractal coefficient and D is the fractal dimension. It can be pointed out that each detected L corresponds to a cell number N_{cell}. Considering average diameter of single cells is 6 μm, each chord length which is lesser than 6 μm ($i = 3$) corresponds to one single cell. To summarize, cell numbers (N_{obs}) measured by laser particle analyzer can be expressed as equation (5). N_{obs} is a constant when cell concentration is equal.

$$N_{obs} = \sum_{i=1}^{3} b_i + \sum_{i=3}^{500} b_i A_D L_i^D \tag{5}$$

Porosity can be expressed by transformed equation (3)

$$\sigma = 1 - \frac{4A_D L^{D-2}}{\pi} \quad (6)$$

Then, average porosity is obtained.

$$\overline{\sigma} = \frac{\sum_{i=1}^{500} \sigma_i L_i b_i}{\sum_{i=1}^{500} L_i b_i} \quad (7)$$

2.5. The Sedimentation of Flocs

Flocculating yeast was rinsed using 0.1 mol L^{-1} EDTA solution once and deionized water twice then dispersed in 500 mL deionized water, adjusted cell dry weight to 10, 20, 30 g L^{-1}, and 0.01 mol L^{-1} $CaCl_2$ was added to trigger flocculation. Floc size was monitored by FBRM and was adjusted to d_0 via tuning the rotation. Right after the stirring stopped, the position of the flocs-water interface was recorded over time.

2.6. Simulation of Flocs Sedimentation

A total of 1000 cells were added to a 2-D space with 1000 × 400 grids and formed various flocs with initial particle size 5, 10, 20 μm. The settlement height where 90% cells below were recorded. During the sedimentation of flocculating cells, flocs aggregate to make larger flocs that settle at a higher speed. However, higher cell concentration imposes higher resistance, which slows the flocs down as they subside. In this way, dynamic equations of flocs sedimentation should include an accelerate term brought by floc growth and a decelerate term brought by compressive sediment in addition to that of particle sedimentation in static water.

Dynamic equations of particles in static water satisfy equation (8)[27]:

$$v = Gd^n \quad (8)$$

v is the settling velocity, G and n were settling parameters varied with flow conditions as shown in Table S1, Supporting Information.

Three factors contribute to collisions among flocs: perikinetic flocculation caused by Brownian movement, orthokinetic flocculation caused by turbulence, and differential settling. All three were considered in the computer simulation of sedimentation in static water.

3. Results and Discussion

3.1. Simulated Flocs Share the Similar Properties With Actual Flocs

Formation of flocs was demonstrated in both 2D and 3D virtual simulations (Videos 1 and 2, Supporting Information).

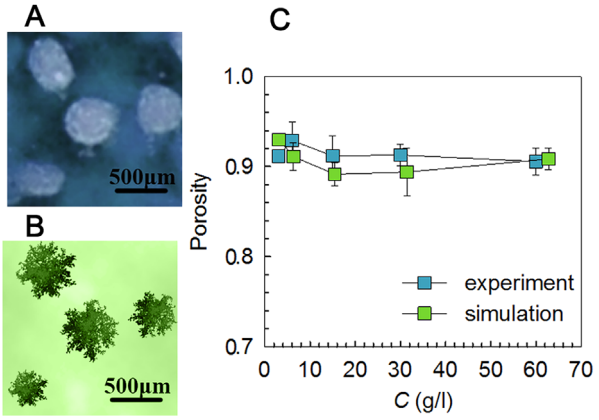

Figure 1. The morphology and porosity of real and simulated flocs. A) Real-time photo of yeast flocs was captured by a digital camera in a stirred fermenter; (B) Virtual yeast flocs was generated by DLA model in a 3-dimension space; (C) The porosity of real flocs was calculated based on chord distribution by FBRM (Equation 7), and porosity of simulated flocs was provided by DLA model (Equation 3). All results are presented as mean and standard deviations (error bar) of triplicated independent experiments or simulation.

The 2D-simulation presented the formation process, but its shape was very different from the real flocs (**Figure 1**A). However, the 3D-simulation illustrated the similar morphological appearance when compared to the actual flocs with a central symmetric sphere (Figure 1B). Moreover, the fractal parameters were calculated through fitting equations 4 and 5 and are shown in **Table 1**. Good performance of the fitting indicated that flocs formed by flocculating yeast satisfied to fractal characters.

Average porosity of the experimental flocs was estimated by substituting fractal parameters obtained by FBRM monitor to the equations 6 and 7, and it was shown that both flocs from experiment and simulation have the similar porosity (Figure 1C). The DLA simulated flocs also complied with fractal characters.[28] In summary, both simulated and experimental flocs had similar fractal structures, as well as their porosities and appearances, were also similar. Therefore, the method of exploring structures of actual flocs by simulating virtual flocs from DLA model presented in this paper was feasible.

3.2. Connection Force and Shear Force Shape the Morphology of Flocs

The flocs are mainly built by the connection forces and destroyed by the shear forces. Connection forces among flocculating yeast cells are mainly conferred by the interactions between proteins and sugar residues on the surface of cellular walls,[29] which was represented by absorption factor (a) in the DLA model. As shown in **Figure 2**A, under the effect of same shear force, higher the value of a, larger the floc size would be, but a variation of a showed little effect on the porosity. Certain particle size was maintained by the equilibrium of disintegration caused by shear force and the growth of floc itself. It was revealed that size of flocs became larger with the decreasing rotation (Figure 2B) which may be attributed to the decreased shear force. Simulations

Table 1. Fractal parameters for different cell concentration.

$C^{a)}$	$C_N{}^{b)}$	A_D	D	R^2
0.6	0.00228	1.224	1.245	0.982
3	0.0114	1.227	1.511	0.989
6	0.0228	1.504	1.498	0.994
15	0.057	1.806	1.566	0.991
30	0.114	1.478	1.780	0.992
60	0.228	1.449	1.833	0.992

[a)] Cell dry weight ($g\,L^{-1}$). [b)]Simulated cell concentration.

based curves showed a quite similar trend to size-rotation when compared to the curves obtained by FBRM. Therefore, the floc-size distribution could be controlled by setting the stirring speeds.[30] However, a variation of shear force due to rotation speed did not make a notable impact on the porosity of flocs. It means that the size of the flocs can be controlled without disturbing the porosity, where porosity is important in terms of efficient mass transfer particularly for the cells present in the core of the floc.

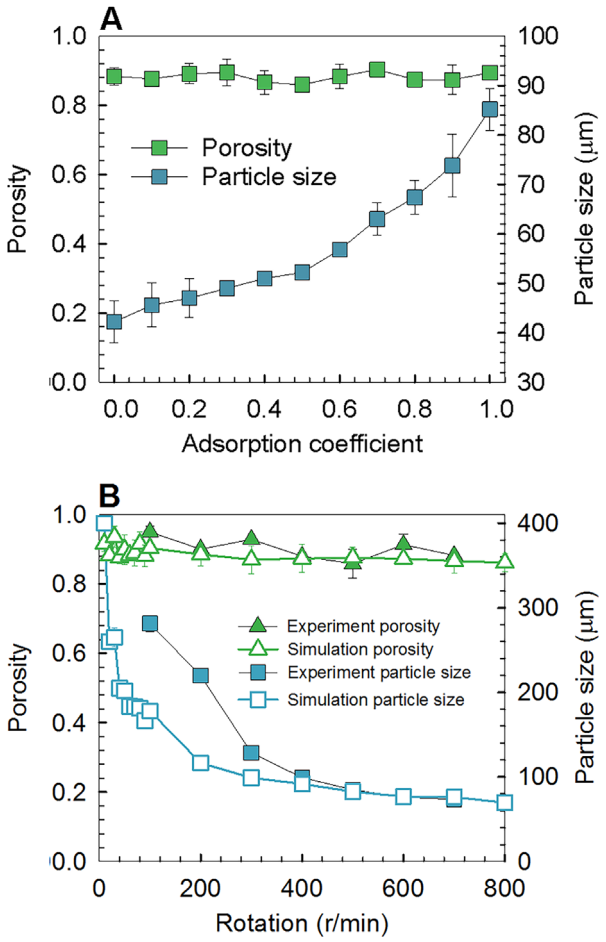

Figure 2. Effects of DLA model parameters on flocs particle size and porosity. A) adsorption coefficient; (B) rotation; Simulated cell concentration C_N was 0.08, and the real cell dry weight in a 1 L fermenter was adjust to about $20\,g\,L^{-1}$ (Equation 2). All results are presented as mean and standard deviations (error bar) of triplicated independent experiments or simulation.

3.3. Cell Propagation Facilitates Large and Compact Flocs

So far, the DLA flocs from flocculating cells are similar with other flocs from abiotic particles such as the colloid.[31] It is interesting to note that the live yeast cells are still able to proliferate in the flocs along with ethanol production. The pores in the core of flocs were thus being occupied directly by newborn yeast cells. It was shown that once simulated cell concentration was invariant, flocs containing proliferating cells were more condensed than those which do not contain dividing cells and flocs were simply formed by mere cell collisions (**Figure 3**A).

During flocculation, the regeneration and disintegration also happened. Keeping the shear force constant, a higher specific growth rate resulted in the formation of bigger, stable, and less porous flocs (Figure 3B). In other words, compactness signifies the mechanical strength of flocs, which could endure the destructive impact of shear force and allows the formation of larger aggregates. Ge et al. have investigated the effect of biomass on floc size distribution, which showed the same phenomenon that more biomass makes the flocs to become bigger.[17]

In fact, flocs produced by flocculating yeast cells during cultivation in shake flasks and fermentation in stirring bioreactor significantly were shown to be in accordance with the cell proliferation DLA model (Figure S2, Supporting Information). In shaking flask, the shear force was milder and cells grew faster, thus flocculating yeast inclined to compose into large and dense flocs. However, in fermenter during continuous ethanol fermentation, since high ethanol imposed a feedback inhibitory impact on cell regeneration for a long time, the decreased cell growth rate resulted in smaller flocs despite constant shear force.

The faster growth of flocculating yeast not only contributed to quick biomass accumulation for high efficient bioconversion but also allowed the formation of stable flocs with larger size and lower porosity, which facilitates sedimentation after fermentation. Whereas, the mass transfer might be a severe problem for inner cells with the increase of floc size and a decrease of porosity. Therefore, a new way to modulate the morphological characters of flocs is required to control cell growth rate through environmental factors including aeration, pH, and temperature. For instance, redox potential control can determine yeast cell's growth rate and floc size simultaneously.[32]

The basic DLA model works well for the non-live system, where the structure of flocs keeps stable once the environmental factors such as shear force, absorption force are fixed. However, the reproduction of live yeast makes the flocs more complicated. Compared with other models, modified DLA model considering the cell propagation is unique in flocculating cells system, which benefits to evaluate the internal mass transfer and process control based on cell growth.

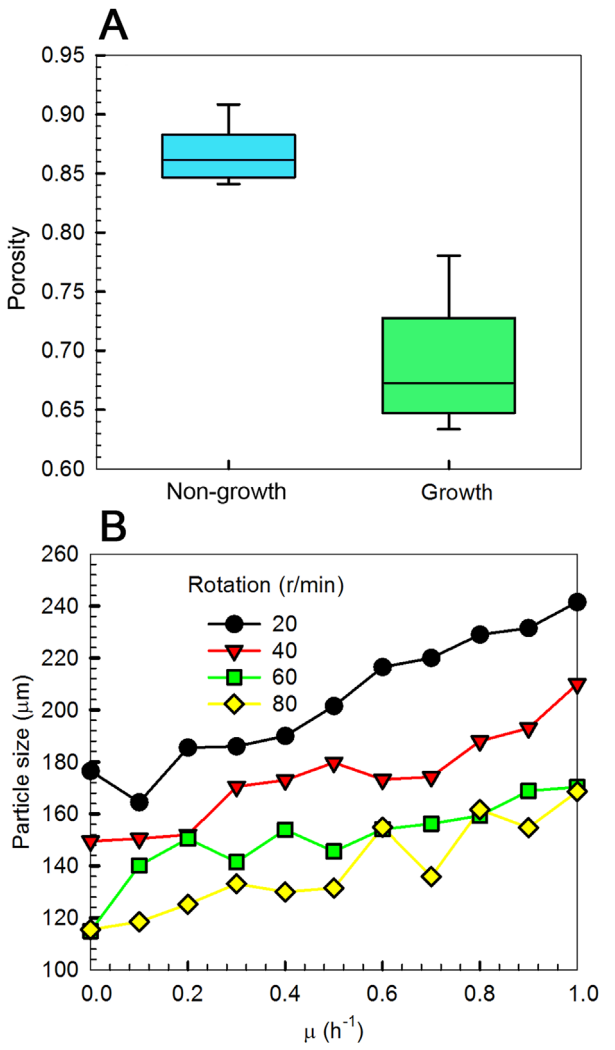

Figure 3. The properties of flocs with cell proliferation. A) Porosity of flocs were simulated under the specific growth rate μ 0 h^{-1} for non-growth cell and 0.5 h^{-1} for growth cell, and no shear force was involved; (B) Particle size of flocs was calculated when considering cell growth (μ: 0–1 h^{-1}) and shear force (rotation: 20–80 r min^{-1}) simultaneously. All results are presented as mean and standard deviations (error bar) of triplicated independent experiments or simulation.

3.4. Simulation of Sedimentation for Multi-Flocs

In order to describe the real flocs behaviors in fermenters, we upgraded the single floc DLA simulation to the multiple flocs model that combined formation and interaction of flocs simultaneously, instead of using the empirical equation in a macro view, which is different from Salim et al.[33] Moreover, the gravity was also considered to illustrate the sedimentation in static water induced by cell flocculation (Figure S3, Supporting Information).

Sedimentation of flocs underwent two phases including the acceleration phase and the deceleration phase. At the beginning, the cells were shown to keep very small floc size due to agitation in the fermentor. As soon as the stirring was stopped, flocs settled in the response to gravity and aggregated with surrounding cells, which enlarged floc size and accelerated sedimentation. All flocs get bigger until reached the bottom and finally are converted into one super-floc. Afterwards, a local cell concentration is increased in the bottom of the fermenter, which prevents the cell layer from becoming thinner. Simulation of sedimentation (Videos 3, 4, and 5, Supporting Information) indicated the simplified accelerated settlement process. The initial floc size, after the stirring was stopped, significantly determined the settling time. Because the flocs with large size could easily go down by gravity, and at the same time, big flocs

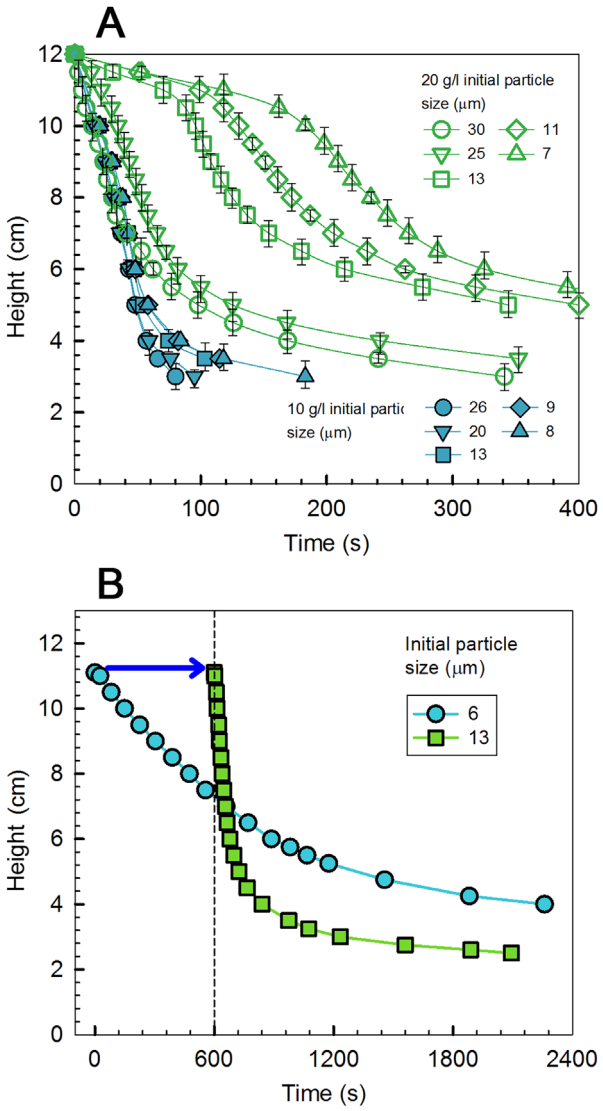

Figure 4. Sedimentation profiles of real flocs. A) Time-course settlement height for yeast flocs at different initial particle sizes and cell concentrations. B) A strategy to enhance the sedimentation: decreasing rotation from 300 to 250 r min^{-1} in 10 min with the enlargement of floc size from 6 μm (blue) to 33 μm (green), and big flocs settled down quickly after stirring stop. All results are presented as mean and standard deviations (error bar) of triplicated independent experiments or simulation.

have more possibility to adhere to other smaller flocs to enlarge itself.

A time-course falling position of sediment interface is shown in **Figure 4**A. It was revealed that cell concentration mainly contributed to a shift in the inflection point of settling profiles. Particles seldom interfere mutually when cell concentration is quite low, in which case their sedimentation can be treated as a free settlement. But when cell concentration is high enough, particles settle slower than in free settlement due to their interaction.[34] Ggreater the biomass, denser the sediment layer would be. Thus it was shown that deceleration began at 4 cm (10 g L^{-1}), over 6 cm (20 g L^{-1}), respectively. Initial floc size also had an important impact on settling time, especially at higher cell concentration level. For 10 g L^{-1}, flocculation curves with different initial floc sizes were almost the same. For 20 g L^{-1}, the sedimentation profiles showed significant differences in response to various initial floc size. For instance, to get a settlement height 6 cm, yeast cell with 30 μm initial floc size took only 90 s, and 7 μm took 400 s (fivefold longer). Bigger initial flocs facilitated to capture more small flocs in high cell concentration condition and led to rapid sedimentation. It can be concluded that the sedimentation of flocs was quite dependent on cell concentrations and initial floc size distributions. Conclusively, a lower cell concentration and a bigger initial floc size attributed to a rapid sedimentation.

Although the reasonable cell concentration is a premise for suitable settling, however, this parameter is usually not a flexible in industrial design. Initial floc size features ann important role in sediment, which can be regulated by changing the stirring speed. It may be concluded that low-speed stirring should be provided to the flocculation system before settling instead of a sudden stop, which will allow the smaller flocs to grow larger enough. A comparison of regular sedimentation and sedimentation after floc growth was made in a system whose cell concentration was 30 g L^{-1} and average floc size was 6 μm (Figure 4B). Average size increased from 6 to 33 μm by reducing the stirring speed during the last 10 min. Although growth of flocs spent 10 min, the total settling time was still shorter than that without floc growth. In addition, the thickness of sedimentation layer was also reduced from about 4 to 3 cm. Taking together all these premises, this strategy is a considerably time-saving and efficient separation method.

4. Conclusion

Yeast cell flocs were simulated based on DLA model to explain structures and sedimentation properties. The cell adsorption can increase floc size, while shear force had an opposite effect. But neither had a significant impact on the porosity of flocs. Cell proliferation can make flocs less porous, and then flocs will be mechanically stronger and larger. Therefore, enhancing cell interaction, maintaining mild shear force, and boosting cell growth will favor the formation of larger flocs. The sedimentation simulation indicated that big initial floc size can accelerate sedimentation. A strategy to achieve efficient sedimentation based harvesting is thus proposed. Due to the lack of direct tools to depict in-situ flocs structure online, we proposed a modified DLA model to construct the numerical flocs, which contributed to unveil the structural mechanism of cell flocculation and consequently carry out rational engineering design to control flocculation for improvement of biorefinery.

Abbreviations

DLA, diffusion-limited aggregation; FBRM, Focused Beam Reflectance Measurement.

Supporting Information

Supporting Information is available from the Wiley Online Library or from the author.

Acknowledgements

This work was supported by the National Natural Science Foundation of China (21536006, 21406030, and 51561145014).

Conflict of Interest

The authors declare no financial or commercial conflict of interest.

Nomenclature

A [−]	flocculation coefficient
A_D [−]	fractal coefficient
b [−]	counts of chord length
C [g L^{-1}]	cell dry weight
C_N [−]	simulated cell concentration
D [−]	fractal dimension
d [μm]	floc size
g [s^{-2}]	gravity
L [μm]	chord length
N [−]	number of flocs
N_{cell} [−]	number of cells
N_{new} [−]	the number of newly regenerated cells
N_{total} [−]	the number of total cells
Re [−]	Reynolds number
S [μm^2]	space area
t [s]	time
v [cm s^{-1}]	sedimentation speed

Greek symbols α [−] Absorption factor

ρ [g cm^{-3}]	density
η [−]	viscosity of water
μ [h^{-1}]	specific growth rate
σ [−]	porosity

Subscript

s [−]	solid
l [−]	liquid

obs [−]observation
c [−] cells

Keywords

DLA model, floc, flocculation, sedimentation, simulation, yeast

Received: November 14, 2017
Revised: December 31, 2017
Published online: January 31, 2018

[1] X. Q. Zhao, F. W. Bai, *Biotechnol. Adv.* **2009**, *27*, 849.
[2] R. Tofalo, G. Perpetuini, P. Di Gianvito, G. Arfelli, M. Schirone, A. Corsetti, G. Suzzi, *J. Appl. Microbiol.* **2016**, *120*, 1574.
[3] P. Di Gianvito, C. Tesnière, G. Suzzi, B. Blondin, R. Tofalo, *Sci. Rep.* **2017**, *7*, 10786.
[4] N. Zhao, Y. Bai, C. G. Liu, X. Q. Zhao, J. F. Xu, F. W. Bai, *Biotech. J.* **2014**, *9*, 362.
[5] C. Wan, M. A. Alam, X. Q. Zhao, X. Y. Zhang, S. L. Guo, S. H. Ho, J. S. Chang, F. W. Bai, *Bioresource Technol.* **2015**, *184*, 251.
[6] F. W. Bai, W. A. Anderson, M. Moo-Young, *Biotechnol. Adv.* **2008**, *26*, 89.
[7] K. J. Verstrepen, G. Derdelinckx, H. Verachtert, F. R. Delvaux, *Appl. Microbiol. Biotechnol.* **2003**, *61*, 197.
[8] R. A. Speers, Y. Q. Wan, Y. L. Jin, R. J. Stewart, *J. Inst. Brew.* **2006**, *112*, 246.
[9] X. M. Ge, F. W. Bai, *J. Biotechnol.* **2006**, *124*, 363.
[10] B. Oyegbile, P. Ay, S. Narra, *Environ. Eng. Res.* **2016**, *21*, 1.
[11] I. Lou, I. In Ieong, *Environ. Model Assess* **2015**, *20*, 225.
[12] A. J. Manning, J. V. Baugh, J. R. Spearman, R. J. S. Whitehouse, *Ocean Dynam.* **2010**, *60*, 237.
[13] F. Mietta, C. Chassagne, R. Verney, J. C. Winterwerp, *Ocean Dynam.* **2011**, *61*, 257.
[14] R. K. Chakraborti, J. F. Atkinson, J. E. Van Benschoten, *Environ. Sci. Technol.* **2000**, *34*, 3969.
[15] S. Lambert, S. Moustier, P. Dussouillez, M. Barakat, J. Y. Bottero, J. Le Petit, P. Ginestet, *J. Colloid Interface Sci.* **2003**, *262*, 384.
[16] O. S. Agimelen, A. Jawor-Baczynska, J. McGinty, J. Dziewierz, C. Tachtatzis, A. Cleary, I. Haley, C. Michie, I. Andonovic, J. Sefcik, A. J. Mulholland, *Chem. Eng. Sci.* **2016**, *144*, 87.
[17] X. M. Ge, X. Q. Zhao, F. W. Bai, *Biotechnol. Bioeng.* **2005**, *90*, 523.
[18] A. R. Heath, P. D. Fawell, P. A. Bahri, J. D. Swift, *Part. Systems Char.* **2002**, *19*, 84.
[19] S. Sun, M. Weber-Shirk, L. W. Lion, *Environ. Eng. Sci.* **2015**, *33*, 25.
[20] T. A. Witten, L. M. Sander, *Phys. Rev. Lett.* **1981**, *47*, 1400.
[21] B. A. Legg, M. Zhu, L. R. Comolli, B. Gilbert, J. F. Banfield, *Langmuir.* **2014**, *30*, 9931.
[22] W. Sun, W. Wang, Y. Gu, X. Xu, J. Gong, *Fuel.* **2017**, *191*, 106.
[23] C. S. Lee, J. Robinson, M. F. Chong, *Process Saf. Environ.* **2014**, *92*, 489.
[24] X. Shen, J. P. Y. Maa, *Mar. Geol.* **2016**, *379*, 84.
[25] D. N. Thomas, S. J. Judd, N. Fawcett, *Water Res.* **1999**, *33*, 1579.
[26] R. K. Chakraborti, K. H. Gardner, J. F. Atkinson, J. E. Van Benschoten, *Water Res.* **2003**, *37*, 873.
[27] J. C. Winterwerp, *Cont. Shelf Res.* **2002**, *22*, 1339.
[28] F. L. Braga, O. A. Mattos, V. S. Amorin, A. B. Souza, *Physica A* **2015**, *429*, 28.
[29] K. V. Y. Goossens, F. S. Ielasi, I. Nookaew, I. Stals, L. Alonso-Sarduy, L. Daenen, S. E. Van Mulders, C. Stassen, R. G. E. van Eijsden, V. Siewers, F. R. Delvaux, S. Kasas, J. Nielsen, B. Devreese, R. G. Willaert, *mBio* **2015**, *6*, e00427.
[30] X. M. Ge, L. Zhang, F. W. Bai, *Enzyme Microb. Tech.* **2006**, *39*, 289.
[31] D. Wang, R. Wu, Y. Jiang, C. W. K. Chow, *Colloids Surf. A* **2011**, *379*, 36.
[32] C. G. Liu, X. M. Hao, Y. H. Lin, F. W. Bai, *Sci. Rep.* **2016**, *6*, 25763.
[33] S. Salim, L. Gilissen, A. Rinzema, M. H. Vermuë, R. H. Wijffels, *Bioresource Technol.* **2013**, *144*, 602.
[34] G. W. Tsou, R. M. Wu, P. S. Yen, D. J. Lee, X. F. Peng, *J. Colloid Interface Sci.* **2002**, *250*, 400.

